GHR1 Zircon – A New Eocene Natural Reference Material for Microbeam U-Pb Geochronology and Hf Isotopic Analysis of Zircon

Michael P. **Eddy** (1,2)* iD, Mauricio **Ibañez-Mejia** (1,3)* iD, Seth D. **Burgess** (4), Matthew A. **Coble** (5) iD, Umberto G. **Cordani** (6), Joel **DesOrmeau** (7) iD, George E. **Gehrels** (8), Xianhua **Li** (9), Scott **MacLennan** (2) iD, Mark **Pecha** (8), Kei **Sato** (6), Blair **Schoene** (2) iD, Victor A. **Valencia** (10) iD, Jeffrey D. **Vervoort** (10) and Tiantian **Wang** (11)

(1) Department of Earth, Atmospheric and Planetary Sciences, Massachusetts Institute of Technology, 77 Massachusetts Ave., Cambridge, MA 02139, USA
(2) Department of Geosciences, Princeton University, Guyot Hall, Princeton, NJ 08544, USA
(3) Department of Earth and Environmental Sciences, University of Rochester, Rochester, NY 14627, USA
(4) U.S. Geological Survey, 345 Middlefield Road, Mail Stop 910, Menlo Park, CA 94025, USA
(5) Department of Geological Sciences, Stanford University, Stanford, CA 94305, USA
(6) Institute of Geosciences, University of São Paulo, Rua do Lago, 562, São Paulo CEP 05508-080, Brazil
(7) Department of Geological Sciences, University of Nevada, Reno, NV 89557, USA
(8) Department of Geosciences, University of Arizona, 1040 E. 4th Street, Tucson, AZ 85721, USA
(9) State Key Laboratory of Lithospheric Evolution, Institute of Geology and Geophysics, Chinese Academy of Sciences, Beijing 100029, China
(10) School of the Environment, Washington State University, Pullman, WA 99164, USA
(11) State Key Laboratory of Biogeology and Environmental Geology, China University of Geosciences, Beijing 100083, China
* Corresponding authors. e-mails: meddy@princeton.edu and ibanezm@rochester.edu

We present multitechnique U-Pb geochronology and Hf isotopic data from zircon separated from rapakivi biotite granite within the Eocene Golden Horn batholith in Washington, USA. A weighted mean of twenty-five Th-corrected $^{206}Pb/^{238}U$ zircon dates produced at two independent laboratories using chemical abrasion-isotope dilution-thermal ionisation mass spectrometry (CA-ID-TIMS) is 48.106 ± 0.023 Ma (2*s* analytical including tracer uncertainties, MSWD = 1.53) and is our recommended date for GHR1 zircon. Microbeam $^{206}Pb/^{238}U$ dates from laser ablation-inductively coupled plasma-mass spectrometry (LA-ICP-MS) and secondary ion mass spectrometry (SIMS) laboratories are reproducible and in agreement with the CA-ID-TIMS date to within < 1.5%. Solution multi-collector ICP-MS (MC-ICP-MS) measurements of Hf isotopes from chemically purified aliquots of GHR1 yield a mean $^{176}Hf/^{177}Hf$ of 0.283050 ± 17 (2*s*, *n* = 10), corresponding to a εHf_0 of +9.3. Hafnium isotopic measurements from two LA-ICP-MS laboratories are in agreement with the solution MC-ICP-MS value. The reproducibility of $^{206}Pb/^{238}U$ and $^{176}Hf/^{177}Hf$ ratios from GHR1 zircon across a variety of measurement techniques demonstrates their homogeneity in most grains. Additionally, the effectively limitless reserves of GHR1 material from an accessible exposure suggest that GHR1 can provide a useful reference material for U-Pb geochronology of Cenozoic zircon and Hf isotopic measurements of zircon with radiogenic $^{176}Hf/^{177}Hf$.

Keywords: U-Pb geochronology, zircon, reference material, Hf isotope ratios, ID-TIMS, LA-ICP-MS, secondary ion mass spectrometry, MC-ICP-MS.

U-Pb zircon geochronology is a versatile and widely used technique to generate dates from the Hadean to the Pleistocene. Microbeam U-Pb zircon geochronology by LA-ICP-MS and SIMS has increasingly been used to address a variety of problems, including the provenance of sediments (e.g., Gehrels 2014 and references therein), the timescales of magmatic processes (e.g., Guillong *et al.* 2014, Padilla *et al.* 2016, Zimmerer *et al.* 2016), timing and rates of metamorphic processes (e.g., Vorhies *et al.* 2013, Viete *et al.* 2015) and, when combined with Hf-in-zircon isotopic measurements,

crustal evolution (e.g., Dhuime *et al.* 2012, Roberts and Spencer 2015, Bauer *et al.* 2017). Techniques for microbeam zircon geochronology and Hf isotopic measurements provide much faster analysis time, higher spatial resolution and are less destructive than traditional bulk dissolution (± isotope dilution). However, microbeam methods require matrix-matched reference materials to correct measured U-Pb and Hf isotopic ratios for instrumental fractionation and to assess reproducibility (e.g., Black *et al.* 2004, Jackson *et al.* 2004). Primary reference materials for calibration of U-Pb and Hf isotopic ratios are now widely available and are typically subsampled from large, homogenous zircon crystals (e.g., Wiedenbeck *et al.* 1995, Jackson *et al.* 2004, Gehrels *et al.* 2008, Kennedy *et al.* 2014). However, the availability of compositionally diverse secondary reference materials that span a variety of ages and Hf isotopic compositions remains limited. These materials are needed to evaluate reproducibility and are particularly limited for Cenozoic zircon (Table 1). This limitation is due, in part, to the ability to distinguish subtle age heterogeneity in zircons of this age. Nevertheless, secondary reference materials of this age are needed as microbeam U-Pb geochronology of Cenozoic zircon becomes more common.

Ideal secondary zircon reference materials for microbeam analysis are homogenous with respect to U-Pb and Hf isotopic compositions, similar in age and Hf isotopic composition to the unknowns of interest, have variable composition to test matrix effects and isobaric interference corrections, and abundant and easily available. We present U-Pb and Hf isotopic data from a proposed natural zircon reference material of Eocene age, GHR1. The U-Pb and Hf isotopic data are reproducible across a variety of methods, and we discuss the merits and limitations of this potential reference material below.

Geological setting and sample description

The Golden Horn batholith is a large, Eocene-aged, epizonal intrusive complex exposed in the North Cascades, USA (Figure 1a). It is composed of several large sills that range in composition from peralkaline granite to calc-alkaline granite and granodiorite (Figure 1b: Stull 1969, Eddy *et al.* 2016). Al-in-hornblende barometry suggests that the batholith intruded at ~ 0.25 GPa, and U-Pb zircon data indicate rapid emplacement over 739 ± 34 ka at ~ 48 Ma (Eddy *et al.* 2016). The largest intrusive phase within the Golden Horn batholith is a > 424 km^3 sill of biotite granite and granodiorite with a distinctive rapakivi texture (Stull 1969, 1978). Existing U-Pb zircon geochronology from this unit shows no resolvable dispersion in Th-corrected ^{206}Pb/^{238}U

dates within individual samples and no resolvable age dispersion between geographically disparate samples (Eddy *et al.* 2016). Given this apparent homogeneity in U-Pb zircon dates, we have investigated the suitability of zircon from this unit as a natural reference material for microbeam U-Pb zircon geochronology. We have also investigated the homogeneity of the zircon Hf isotopic compositions from this granite and assessed its suitability as a reference material for microbeam Hf isotopic analyses of zircon.

The studied sample (GHR1) was collected from a road cut through biotite rapakivi granite located ~ 1.1 km west of the Lone Fir US Forest Service Campground along WA State Route 20 (Figure 1: 48.57308°N 120.63125°W) and corresponds to sample NC-MPE-086 in Eddy *et al.* (2016). Zircons from GHR1 are euhedral with aspect ratios 2:5–1:2 and lengths up to 250 μm. Cathodoluminescence (CL) images of select GHR1 zircons were performed at the University of Nevada Reno on a JEOL 7100FT field emission scanning electron microscope using a 10.0 kV beam. The GHR1 grains exhibit oscillatory zoning typical of igneous zircon (Figure 2). Some zircons may have resorption features (Figures 2c, d) that are likely related to complex changes to physical conditions during crystal growth. However, we stress that there is no evidence in the current U-Pb zircon geochronological data set for protracted zircon crystallisation and/or residence times in this unit that are in excess of the analytical uncertainties on individual CA-ID-TIMS analyses (30–90 ky: Eddy *et al.* 2016). Inclusions are common in GHR1 zircon. Energy-dispersive X-ray spectroscopy shows that many of these inclusions are apatite, which may affect the common Pb (Pb$_c$) and rare earth element (REE) contents derived from microbeam analyses. We further discuss the effects of this limitation below.

Method and approach

The purpose of this study was to demonstrate the reproducibility of the U/Pb and Hf isotopic ratios in GHR1 zircon across a wide variety of analytical techniques and data reduction strategies. While standardisation of data acquisition, reduction and reporting is an important step towards increasing reproducibility throughout the U-Pb zircon geochronology and Hf-in-zircon isotopic communities (i.e., Schmitz and Schoene 2007, McLean *et al.* 2011, Condon *et al.* 2015, Horstwood *et al.* 2016), it is not our goal to advocate for specific approaches in this study. Instead, our goal is to illustrate the utility of GHR1 zircon as reference material within the current state of the field. In the sections below, we discuss the analytical conditions and data reduction procedures used within each participating laboratory. Participants include two laboratories that produced U-

Table 1.
Zircon reference materials for microbeam U-Pb and Hf isotopic analyses

Name	ID-TIMS age (Ma) [a]	2s	References [b,c]	$^{176}Hf/^{177}Hf$	2s	References [d,e]	Host lithology	Quantity
Penglai	4.4	0.1	Li et al. (2010) [b]	0.282906	0.000001	Li et al. (2010) [d]	Alkaline Basalt	Unlimited
FCT	28.196–28.638 [f]	–	Wotzlaw et al. (2013) [b]	–	–	–	Dacite	Unlimited
AUS_z2	38.896	0.012	Kennedy et al. (2014) [b]	–	–	–	Single Crystal	Limited
GHR1	48.106	0.023	This Study [c]	0.283050	0.000017	This Study [e]	Rapakivi Granite	Unlimited
Qinghu	159.5	0.2	Li et al. (2009) [b]	0.283002	0.000004	Li et al. (2013) [e]	Quartz Monzonite	Unlimited
Plešovice	337.13	0.37	Sláma et al. (2008) [b]	0.282482	0.000013	Sláma et al. (2008) [d,e]	Potassic Granulite	Unlimited
Temora-1	416.75	0.24	Black et al. (2003) [c]	0.282685	0.000011	Wu et al. (2006) [e]	Gabbroic Diorite	Unlimited
Temora-2	418.37	0.14	Mattinson (2010) [b]	0.282686	0.000008	Woodhead and Hergt (2005) [e]	Gabbro	Unlimited
R33	420.53	0.16	Mattinson (2010) [b]	0.282764	0.000014	Fisher et al. (2014) [d]	Monzodiorite	Unlimited
Z6266	559.0	0.2	Stern and Amelin (2003) [c]	–	–	–	Single Crystal	Limited
SL	563.5	3.2	Gehrels et al. (2008) [c]	0.281630	0.000010	Woodhead and Hergt (2005) [e]	Single Crystal	Limited
Peixe	564	4	Chang et al. (2006) [c]	–	–	–	Alkaline Complex	Unlimited
GJ-1	608.5	1.5	Jackson et al. (2004) [c]	0.282000	0.000005	Morel et al. (2008) [e]	Single Crystal	Limited
Mud Tank	732	5	Black and Gulson (1978) [c]	0.282507	0.000006	Woodhead and Hergt (2005) [e]	Carbonatite	Unlimited
91500	1065.4	0.3	Wiedenbeck et al. (1995) [c]	0.282306	0.000008	Woodhead and Hergt (2005) [e]	Single Crystal	Limited
FC-1	1098.47	0.16	Mattinson (2010) [b]	0.282184	0.000016	Woodhead and Hergt (2005) [e]	Gabbro	Unlimited
OG1	3467.05	0.63	Stern et al. (2009) [b]	–	–	–	Diorite	Unlimited

[a] These dates correspond to those used for standardisation during microbeam analyses as part of this study.
[b] Chemical abrasion (CA)-ID-TIMS.
[c] Traditional ID-TIMS.
[d] Laser ablation MC-ICP-MS.
[e] Solution MC-ICP-MS.
[f] CA-ID-TIMS analyses by Wotzlaw et al. (2013) show significant age dispersion in FCT relative to the original U-Pb ID-TIMS date of Schmitz and Bowring (2001).

Pb ID-TIMS data, one laboratory that produced Hf isotopic data using solution MC-ICP-MS, two laboratories that produced U-Pb and Hf isotopic data by LA-ICP-MS and three laboratories that produced U-Pb SIMS data. All uncertainties are reported at 2s and are explicitly noted as measurement repeatability or reproducibility precision, where appropriate.

U-Pb geochronology

ID-TIMS (MIT and Princeton University)

A total of twenty-one CA-ID-TIMS analyses of single zircons were conducted at the Massachusetts Institute of Technology (MIT: $n = 9$) and Princeton University ($n = 12$) in addition to the six analyses previously published in Eddy et al. (2016). The methods used in each laboratory are slightly modified from Mattinson (2005) and are described in detail in Eddy et al. (2016) for MIT and Samperton et al. (2015) for Princeton University. Twenty-four of the grains were spiked with the EARTHTIME $^{205}Pb-^{233}U-^{235}U$ (ET535) isotopic tracer, and three additional grains were spiked with the EARTHTIME $^{202}Pb-^{205}Pb-^{233}U-^{235}U$ (ET2535) isotopic tracer (Condon et al. 2015, McLean et al. 2015). Isotopic ratios were measured on a VG Sector 54 TIMS at MIT and on a IsotopX Phoenix TIMS at Princeton University.

Instrumental Pb fractionation (α; % amu^{-1}) was calculated using a linear fractionation law from measurements of the $^{202}Pb/^{205}Pb$ ratio in samples spiked with the EARTHTIME $^{202}Pb-^{205}Pb-^{233}U-^{235}U$ (ET2535) isotopic tracer in each laboratory. The resulting $\alpha = 0.182 \pm 0.082$ (2s, $n = 287$) for the IsotopX Phoenix TIMS at Princeton is similar to the value ($\alpha = 0.179 \pm 0.052$, 2s) calculated from repeat measurements of the NBS982 Pb isotopic reference material. However, the mean $\alpha = 0.206 \pm 0.058$ (2s, $n = 53$) for the Sector 54 TIMS at MIT slightly differs from the value ($\alpha = 0.25 \pm 0.04$, 2s) calculated from repeat measurements of the NBS-981 Pb isotopic reference material. For this study,
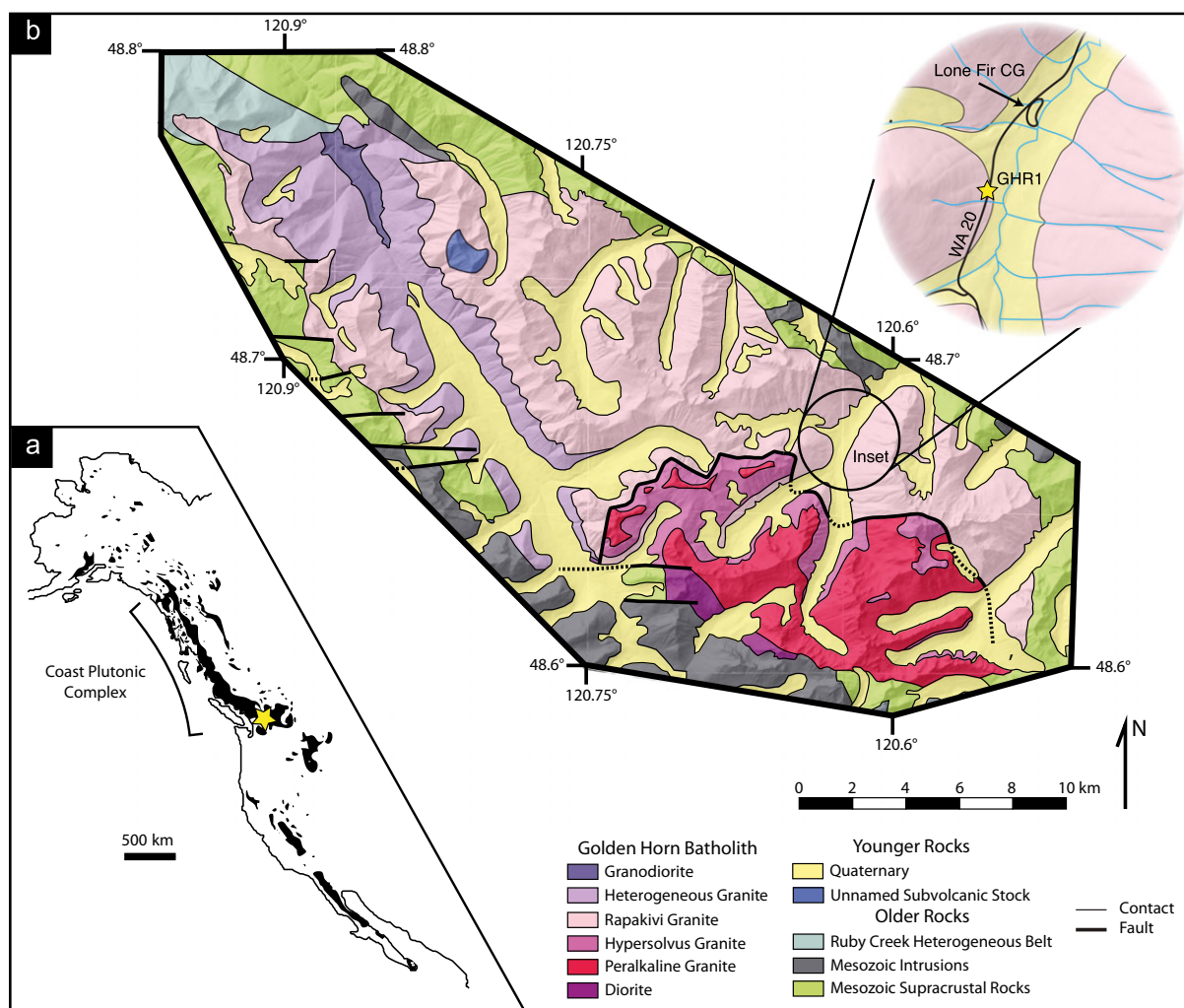
Figure 1. Location maps for the GHR1 sample showing (a) the location of the Golden Horn batholith relative to other granitoids (black) in the North American Cordillera from Miller *et al.* (2000) and (b) the location of the GHR1 outcrop within the Golden Horn batholith. This figure is slightly modified from Eddy *et al.* (2016).

we used the α calculated using measurements of ^{202}Pb/^{205}Pb in zircons spiked with the ET2535 isotopic tracer because they more closely match the running conditions of the unknown zircons. We have also applied this correction to the analyses reported in Eddy *et al.* (2016), which lowers the mean age of this sample by *ca.* 0.4%. For the three grains spiked with the ET2535 isotopic tracer at Princeton University, Pb fractionation was corrected point by point using the known ^{202}Pb/^{205}Pb ratio. Instrumental fractionation of U was internally corrected using the known ratio of ^{233}U/^{235}U in the EARTHTIME ^{205}Pb–^{233}U–^{235}U (ET535) isotopic tracer and assuming a sample ^{238}U/^{235}U = 137.818 ± 0.0225 from the zircon compositions reported by Hiess *et al.* (2012).

Contamination from Pb$_c$ was corrected using laboratory blank isotopic compositions based on procedural blanks and by assuming all measured ^{204}Pb is from laboratory contamination. We consider this assumption to be valid because the mass of Pb$_c$ measured in procedural blanks is similar to that observed during the zircon measurements. A correction for initial secular disequilibrium in the ^{238}U–^{206}Pb decay chain due to preferential exclusion of ^{230}Th during zircon crystallisation (e.g., Schärer 1984) was done using a fractionation factor (f_{ThU} = [Th/U]$_{Zircon}$/[Th/U]$_{Magma}$) of f_{ThU} = 0.138, which is based on zircon and glass geochemical data from high-silica rhyolites from the Yellowstone magmatic system (Stelten *et al.* 2015). Corrected ^{206}Pb/^{238}U dates for individual grains range between 90 and 94 ky older than the uncorrected dates, and the correction has a negligible effect on any potential intergrain age dispersion within the sample. Regardless, we present both Th-corrected and uncorrected values in Tables S1 and S2.
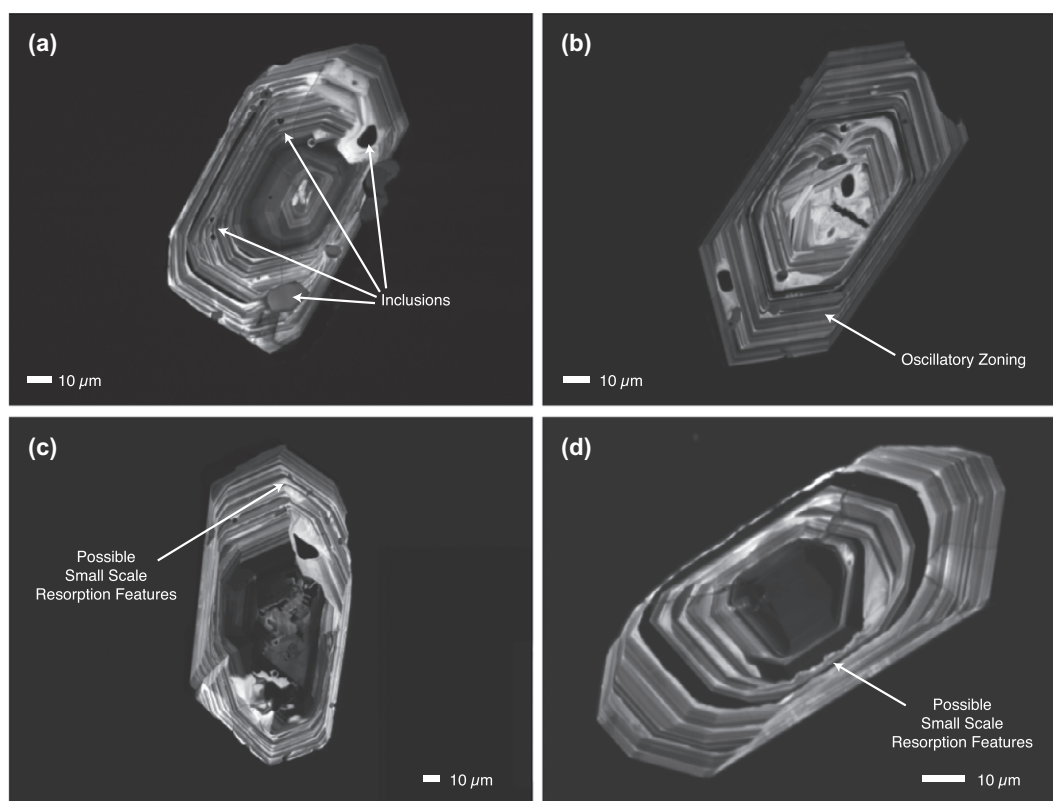
Figure 2. Cathodoluminescence (CL) images of zircon separated from the GHR1 outcrop. Note the oscillatory zoning characteristic of igneous zircon (a–d), possible small-scale resorption features (c, d) and the presence of inclusions (a–c).

All U-Pb isotopic data from the ID-TIMS analyses conducted at MIT and Princeton are presented in Tables 2, Tables S1 and S2 and are shown as concordia plots and as a rank order plot of Th-corrected ^{206}Pb/^{238}U dates in Figure 3. Uncertainties are reported as $2s$ in the format ± A/B/C, where A represents measurement repeatability only, B represents measurement repeatability plus uncertainty in the composition of the ET2535 or ET535 isotopic tracers and C includes propagation of uncertainty in the ^{238}U decay constant. The analyses from MIT show no resolvable age dispersion and give a weighted mean Th-corrected ^{206}Pb/^{238}U date of 48.105 ± 0.011/0.024/ 0.057 Ma (MSWD = 1.52). Ten of the analyses from Princeton University show little age dispersion and give a weighted mean Th-corrected ^{206}Pb/^{238}U date of 48.108 ± 0.014/0.025/ 0.057 Ma (MSWD = 1.70). However, two analyses are distinctly older, with dates of 48.597 ± 0.026 Ma and 50.451 ± 0.098 Ma (2σ analytical uncertainties). We discuss the significance of these grains in the Discussion section. Excluding these two grains, a weighted mean of twenty-five analyses from both Princeton University and MIT gives a Th-corrected ^{206}Pb/^{238}U date of 48.1063 ± 0.0087/0.023/ 0.056 Ma (MSWD = 1.53) and an uncorrected ^{206}Pb/^{238}U date of 48.0133 ± 0.0086/0.023/0.056 Ma (MSWD =

1.57). The weighted mean Th-corrected ^{206}Pb/^{238}U date from the combined data set is our recommended reference date for GHR1 zircon.

A second set of five zircons was analysed by ID-TIMS at Princeton University without using the chemical abrasion procedure to assess the possibility of Pb loss in GHR1 zircon. All analytical methods follow those outlined above for Princeton University, and the results are reported in Table S2 as both Th-corrected and uncorrected data. All of the Th-corrected ^{206}Pb/^{238}U dates for these grains are younger than the reference date reported above (Figure 4), indicating the presence of either younger overgrowths or Pb loss. We discuss the likelihood of these two possibilities in the Discussion section.

LA-ICP-MS (Washington State University)

Twenty-four LA-ICP-MS U-Pb analyses were conducted on polished zircon interiors at Washington State University using a Thermo-Finnigan Element 2 single-collector mass spectrometer coupled with a New Wave Nd:YAG UV 213-nm laser (Table S3). Methods follow those outlined in

Table 2.
Summary of U-Pb geochronology results

Laboratory	Method [a]	No. of analyses	Weighted mean $^{206}Pb/^{238}U$ date (Ma, 2s) [b]	MSWD [c]
MIT	CA-ID-TIMS	n = 15 of 15	48.105 ± 0.024 [d]	1.52
Princeton University	CA-ID-TIMS	n = 10 of 12	48.108 ± 0.025 [d]	1.70
Washington State University	LA-ICP-MS	n = 21 of 24	47.99 ± 0.44 [e]	0.19
University of Arizona	LA-ICP-MS	n = 107 of 114	48.38 ± 0.71 [f]	0.80
Chinese Academy of Sciences	SIMS	n = 25 of 37	48.18 ± 0.31 [f]	0.75
USGS/Stanford	SIMS	n = 18 of 22	48.17 ± 0.35 [e]	1.71
University of Sao Paulo	SIMS	n = 16 of 20	48.70 ± 0.50 [e]	1.50

[a] CA-ID-TIMS: chemical abrasion-isotope dilution-thermal ionisation mass spectrometry, LA-ICP-MS: laser ablation-inductively coupled plasma-mass spectrometry, SIMS: secondary ion mass spectrometry.

[b] All weighted means were calculated using either ET_Redux (Bowring *et al.* 2011) or the MATLAB function included in Appendix S1.

[c] Mean square weighted deviation (Wendt and Carl 1992) calculated using MATLAB function included in the Appendix S1.

[d] CA-ID-TIMS dates include contributions to uncertainty from analytical sources and the calibration of the isotopic tracer.

[e] LA-ICP-MS and SIMS dates from Washington State University, USGS/Stanford and the University of São Paulo include analytical uncertainty only.

[f] LA-ICP-MS and SIMS dates from the University of Arizona and Chinese Academy of Sciences include both measurement repeatability precision and systematic external errors related to reproducibility of zircon reference materials.

Chang *et al.* (2006), and only a brief summary is presented here. Spots were selected using reflected and transmitted light and were 30 μm in diameter. Elemental and mass-fractionation were corrected by bracketing analyses of GHR1 with analyses of Plešovice zircon (Table 1: Sláma *et al.* 2008). Elemental mass fractions were also calibrated relative to this reference material. No correction for contamination with Pb_c was undertaken, and grains that reflect high Pb_c content were not included in the calculation of dates. Data reduction was done using an 'in-house' spreadsheet. Reproducibility was monitored by analysing the 91500 zircon (Table 1: Wiedenbeck *et al.* 1995) and Fish Canyon tuff zircon (Schmitz and Bowring 2001, Wotzlaw *et al.* 2013). Weighted mean $^{206}Pb/^{238}U$ dates and 2s uncertainties for these reference materials are 1065 ± 21 (n = 3, MSWD = 0.22) for 91500 and 27.41 ± 0.64 Ma (n = 4, MSWD = 0.22) for the Fish Canyon tuff. The $^{206}Pb/^{207}Pb$ date for 91500 agrees within uncertainty with the published reference value, while the $^{206}Pb/^{238}U$ date for the Fish Canyon Tuff is *ca.* 4% younger than the range of $^{206}Pb/^{238}U$ CA-ID-TIMS zircon dates for this unit (e.g., Wotzlaw *et al.* 2013). One of the twenty-four analyses of GHR1 was discarded because the grain contained high Pb_c ($^{206}Pb/^{204}Pb$ < 1500). Two additional analyses were also excluded as outliers. These grains gave slightly discordant $^{206}Pb/^{238}U$ dates of 36.5 ± 1.7 Ma (2s) and 40.6 ± 3.1 Ma (2s). We attribute these dates to Pb loss and discuss their significance in the Discussion section. The remaining twenty-one analyses are shown in Figures 5 and 6 and give a weighted mean $^{206}Pb/^{238}U$ date of 47.99 ± 0.44 (0.65) (2s, MSWD = 0.19), where the first uncertainty measurement

repeatability precision and the second incorporates the reproducibility of zircon reference materials within the laboratory.

LA-ICP-MS (University of Arizona)

GHR1 zircons were mounted at the University of Arizona and characterised by CL imaging using a Hitachi 3400N SEM and a Gatan Chroma CL system prior to U-Pb analysis by LA-ICP-MS. A total of 114 laser spots of 20 μm diameter and < 10 μm depth were ablated from ~ 100 polished interiors of GHR1 zircon using an Analyte G2 Photon Machines 193-nm excimer laser and analysed for U-Pb geochronology on a Thermo Element2 ICP-MS at the University of Arizona Laserchron center (Table S4). The methods for these analyses are outlined in Ibañez-Mejia *et al.* (2015) and Pullen *et al.* (2018). GHR1 analyses were bracketed by U-Pb isotopic measurements of fragments from the SL2 (Table 1: Gehrels *et al.* 2008), R33 (Table 1: Black *et al.* 2004) and FC-1 (Table 1: Paces and Miller 1993) zircon reference materials, which were used to correct for elemental- and mass-dependent instrumental fractionation as a function of beam intensity. Mass fractions of U and Th were calibrated relative to zircon reference material SL2 (Gehrels *et al.* 2008). Data reduction was done using an 'in-house' spreadsheet. Pb_c is assumed to be initial (i.e., from co-crystallised inclusions) and is corrected using the measured ^{204}Pb and the isotopic composition of crustal Pb at *ca.* 48 Ma (Stacey and Kramers 1975). Six of the 114 analyses were excluded from our age calculations due to high Pb_c ($^{206}Pb/^{204}Pb$ < 1500). These analyses also exhibit discordance following Pb_c correction that may
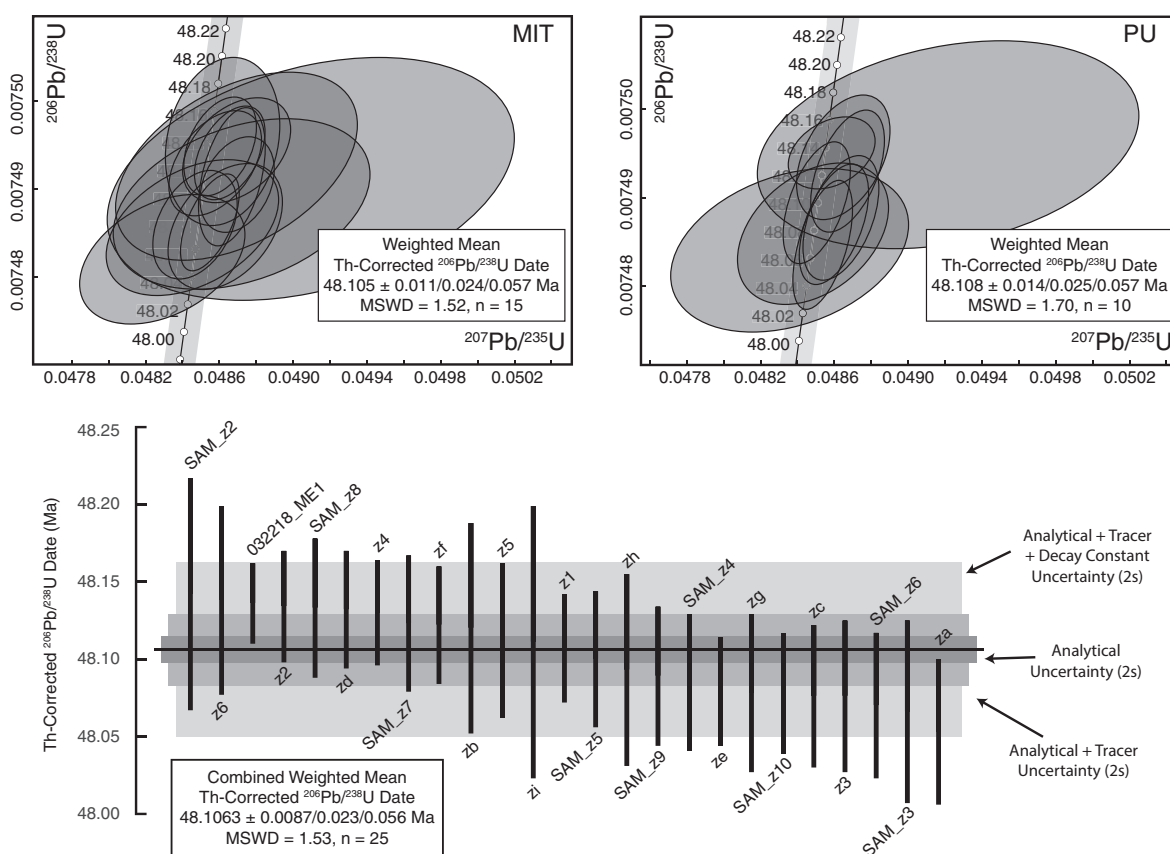
Figure 3. Chemical abrasion-isotope dilution-thermal ionisation mass spectrometry (CA-ID-TIMS) results from MIT and Princeton University. Results are shown as Wetherill concordia plots and as a rank order plot of Th-corrected $^{206}Pb/^{238}U$ dates for the combined data set. Note that two analyses of much older zircon (Table S2) are not shown. All uncertainties are reported as 2s in the format A/B/C, where A represents measurement repeatability precision, B includes the uncertainty in the composition of the isotopic tracer, and C includes uncertainty in the ^{238}U decay constant.

indicate that the Pb_c budget was controlled by surface contamination with modern crustal Pb_c rather than Pb_c incorporated in inclusions during zircon crystallisation (Figure 5). A single analysis that gave a date of 36.7 ± 1.3 Ma (2s) was also excluded as an outlier and is attributed to Pb loss. The remaining 107 $^{206}Pb/^{238}U$ dates are shown in Figure 6 and give a weighted mean date of 48.38 ± 0.19 (0.71) Ma (2s, MSWD = 0.80), where the first uncertainty only represents measurement repeatability precision and the second includes the reproducibility of zircon reference materials measured during the same measurement session.

SIMS (Chinese Academy of Sciences)

Thirty-seven zircons from GHR1 were analysed for U-Pb geochronology on a Cameca IMS-1280HR SIMS at the Institute for Geology and Geophysics at the Chinese National Academy of Sciences. The methods for these

analyses follow those in Li *et al.* (2009). Zircons were first mounted in epoxy, and spots for U-Pb analysis were selected using reflected and transmitted light microscopy. Secondary ions were generated using an O_2^- beam with a diameter of ~ 30 μm and a depth of 2 μm. U-Pb ratios were calibrated by bracketing GHR1 analyses with analyses of the Plešovice zircon reference material (Table 1: Sláma *et al.* 2008), while U and Th mass fractions were calibrated against zircon reference material 91500 (Table 1: Wiedenbeck *et al.* 1995). Long-term reproducibility of these reference materials is 3% (2s), and this uncertainty is propagated to the unknowns following the methods outlined in Li *et al.* (2010). All Pb_c is attributed to surface contamination, and Pb isotopic measurements were corrected for Pb_c using measured ^{204}Pb and the present day crustal Pb isotopic composition from Stacey and Kramers (1975). Data reduction was done using the Cameca Customisable Ion Probe software package using the methods presented in Li *et al.* (2009). The data are reported in Table S5 and shown in Figures 5 and 6. Ten measurements of
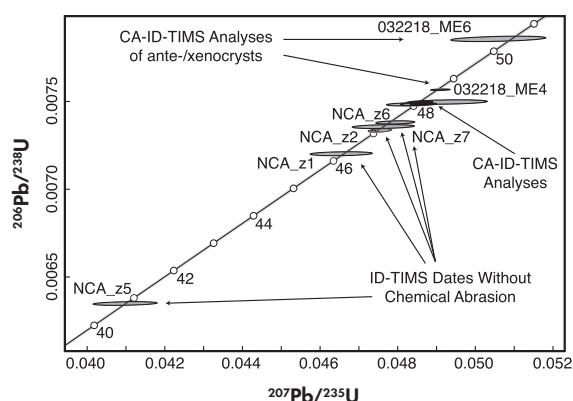
Figure 4. Wetherill concordia plot comparing the results of ID-TIMS analyses of GHR1 zircon that did not undergo chemical abrasion with the CA-ID-TIMS results. All analyses that did not undergo chemical abrasion prior to dissolution are younger than the CA-ID-TIMS analyses, indicating either the presence of younger zircon overgrowths or Pb loss. Note the older CA-ID-TIMS analyses that likely represent ante- or xenocrysts.

Qinghu zircon (Li *et al.* 2013) were conducted to assess reproducibility and have a weighted mean $^{206}Pb/^{238}U$ date of 159.1 ± 1.5 Ma (2*s*, MSWD = 0.47), which is within the uncertainty of the recommended value (Table 1). Twelve of the analyses contained high Pb_c ($^{206}Pb/^{204}Pb$ < 1500) and are excluded from our age calculations. The twenty-five remaining analyses are shown in Figure 6 and give a weighted mean $^{206}Pb/^{238}U$ date of 48.18 ± 0.31 Ma (2σ, MSWD = 0.75), where the reported uncertainty incorporates both measurement repeatability precision and uncertainty related to the long-term reproducibility of zircon reference materials.

SIMS (USGS/Stanford University)

Twenty-two U-Pb measurements were performed on GHR1 zircon using a sensitive high-resolution ion microprobe with reverse geometry (SHRIMP-RG) at the Stanford University. All grains were polished and imaged with reflected light on a petrographic microscope, cleaned by rinsing the mount in dilute hydrochloric acid and distilled water, dried in a vacuum oven and coated with a conductive layer of gold. Zircon U-Pb measurements were performed using an O_2^- primary beam with an intensity ranging from 5.4 to 5.8 nA with analytical spot diameter of ~ 30 μm and a pit depth of ~ 2 μm. Analyses were performed with a mass resolving power of ~ 7000 (10% peak height) to maximise secondary ion transmission and eliminate isobaric

interferences. Measured U/Pb ratios were standardised relative to the Temora-2 zircon (Table 1: Black *et al.* 2004, Mattinson 2010), which was analysed repeatedly throughout the duration of the measurement session. Data reduction follows Ireland and Williams (2003) using the Microsoft Excel add-in programs Squid2.51 (Ludwig 2009). Individual spot analyses are reported as $^{206}Pb/^{238}U$ and $^{207}Pb/^{206}Pb$ dates and were corrected for Pb_c using the measured ^{204}Pb and the crustal Pb_c composition for 48–50 Ma from Stacey and Kramers (1975). All $^{206}Pb/^{238}U$ ages are reported with 2*s* uncertainties, including the uncertainty summed in quadrature from the reproducibility of the Temora-2 reference material during the measurement session. The mass fractions of U and Th were calculated relative to 91500 zircon (Wiedenbeck *et al.* 1995) and MAD-559 zircon (Coble *et al.* 2018). The results of the GHR1 analyses are presented in Table S6 and shown in Figures 5 and 6. Two analyses were excluded from the weighted mean due to high Pb_c ($^{206}Pb/^{204}Pb$ < 1500), and two were excluded because they were outliers. One outlier gave a date of 43.1 ± 1 Ma (2*s*), and the other gave a date of 50.2 ± 1 Ma (2*s*). A weighted mean of the remaining eighteen analyses gave a $^{206}Pb/^{238}U$ date of 48.17 ± 0.35 Ma (2*s*, MSWD = 1.71), where the uncertainty includes both analytical uncertainty and the reproducibility of the Temora-2 reference material during the same measurement session.

A second set of analyses was performed on unpolished surfaces of GHR1 zircon at the USGS/Stanford SHRIMP-RG using the methods described in Matthews *et al.* (2015). The grains were mounted in indium and imaged using a reflected light microscope. Since surface topography can affect mass fractionation in SHRIMP analyses (e.g., Ickert *et al.* 2008, Kita *et al.* 2009), only grains with smooth reflective surfaces were analysed. A total of nineteen surfaces were analysed and yielded $^{206}Pb/^{238}U$ dates ranging from 43.1 to 49.4 Ma (Figure 7). A weighted mean $^{206}Pb/^{238}U$ date for these analyses is 46.69 ± 0.41 Ma (2*s*, MSWD = 4.04), where the uncertainty includes both measurement repeatability precision and the reproducibility of reference materials during the same measurement session. This date is younger than the $^{206}Pb/^{238}U$ date for zircon interiors analysed by the USGS SHRIMP, and the high MSWD indicates that these analyses do not form a coherent population. We discuss the significance of this result in the Discussion section.

SIMS (University São Paulo)

Twenty zircons were analysed using the SHRIMP-IIe at the Institute for Geoscience at the University of Sao Paulo. Zircon grains were mounted with crystals of the Temora-2
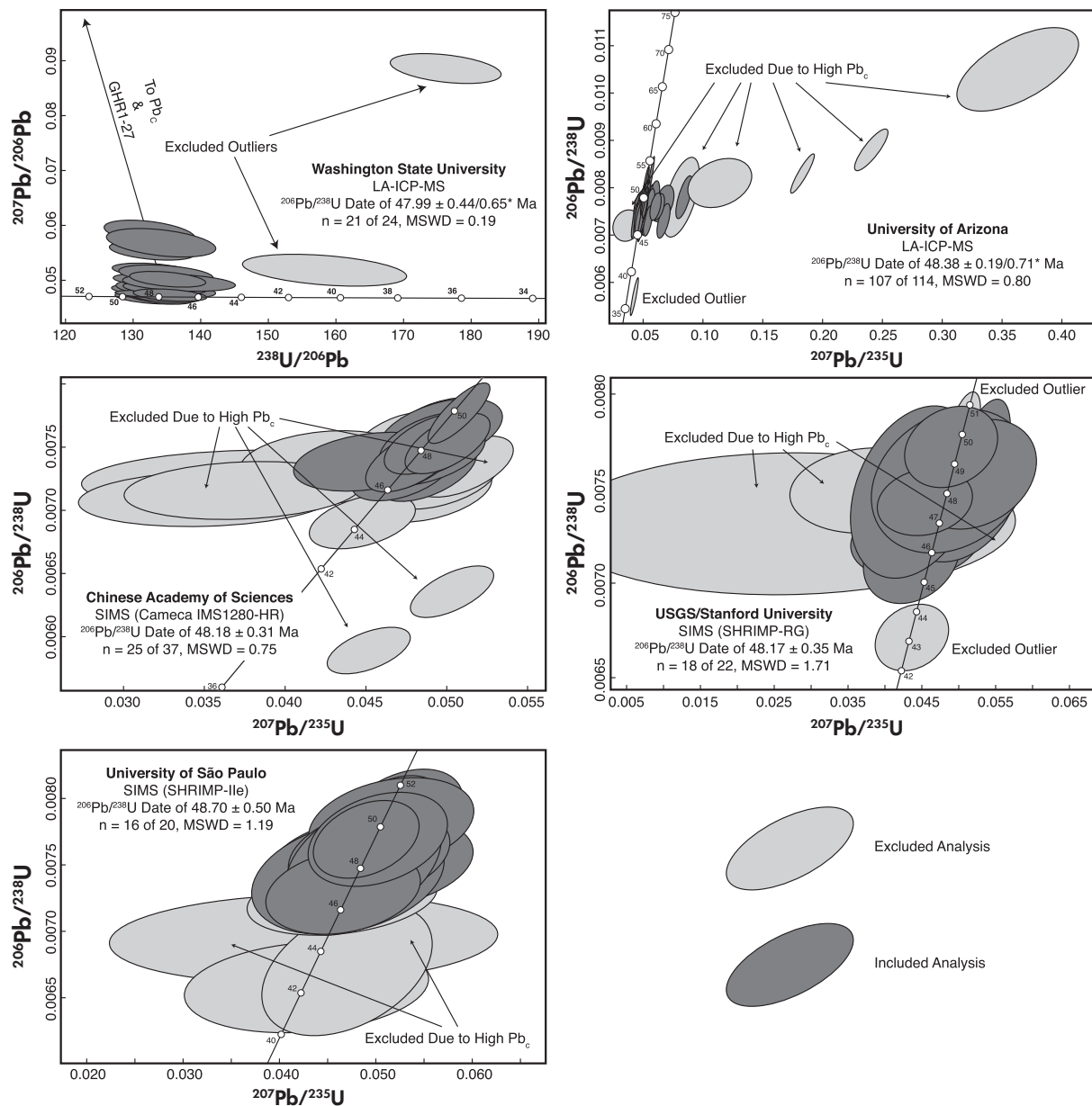
Figure 5. Concordia plots for all microbeam U-Pb analyses by laser ablation-inductively coupled plasma-mass spectrometry (LA-ICP-MS) and secondary ion mass spectrometry (SIMS). The data from Washington State University are not corrected for Pb$_c$ and are shown on a Tera-Wasserburg concordia plot. The rest of the data are corrected for Pb$_c$ using the methods described for each individual laboratory and are shown on Wetherill concordia plots. All dates are reported with 2s uncertainty and mean square weighted deviation (MSWD). *The uncertainty for the dates from the University of Arizona and Washington State University is reported in the format ± A/B, where A represents the measurement repeatability precision and B includes the uncertainty related to the reproducibility of zircon reference materials. Please refer to the text for the uncertainty reporting procedures from each of the other laboratories.

and FC1 zircon reference materials and polished prior to analysis. Cathodoluminescence (CL) images were obtained using a FEI Quanta 250 scanning electron microscope (SEM) and an Oxford Instruments XMAX CL detector in order to identify inclusions and growth domains. After imaging, the

mount was coated in ~ 3 nm of gold and loaded in the SHRIMP-IIe for U-Pb analyses. Analyses were conducted using a ~ 4–5 nA O_2^- beam with a diameter of 30 μm and a raster time of 2.5 min. The zircon reference material Z6266 (Table 1: Stern and Amelin 2003) was used to
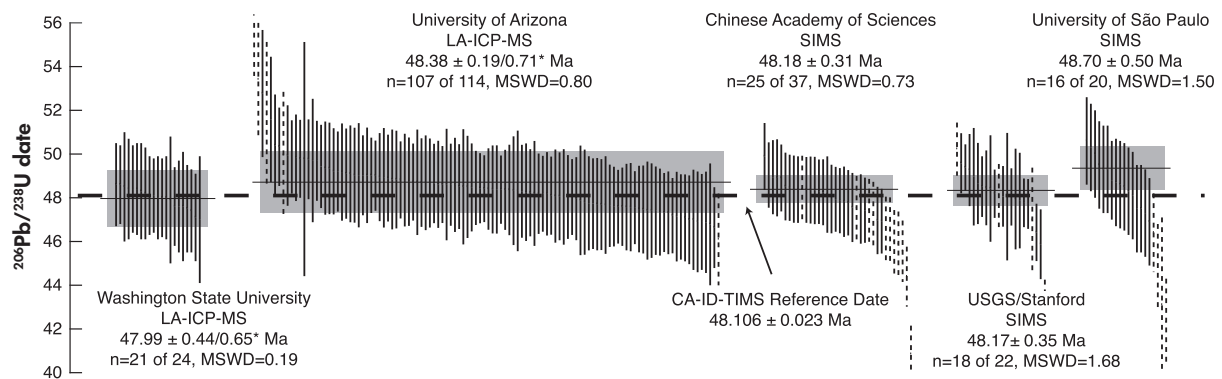
Figure 6. Rank order plot comparing the $^{206}Pb/^{238}U$ dates from microbeam U-Pb measurements relative to the preferred crystallisation date for GHR1 determined by chemical abrasion-isotope dilution-thermal ionisation mass spectrometry (CA-ID-TIMS). Individual bars represent single analyses and are shown with 2*s* uncertainty. Weighted mean dates are also reported with 2*s* uncertainty. Dashed lines were excluded from the weighted mean calculation and correspond to grains with high Pb$_c$ or grains that were outliers. Only data between 56 and 40 Ma are shown. The mean and 2*s* uncertainty for each laboratory are shown as thin black lines and grey boxes, respectively. *The uncertainty for the dates from the University of Arizona and Washington State University is reported in the format ± A/B, where A represents the measurement repeatability precision and B includes the uncertainty related to the reproducibility of zircon reference materials. Only the full uncertainty (B) is shown on the figure. Please refer to the text for the uncertainty reporting procedures from each of the other laboratories.
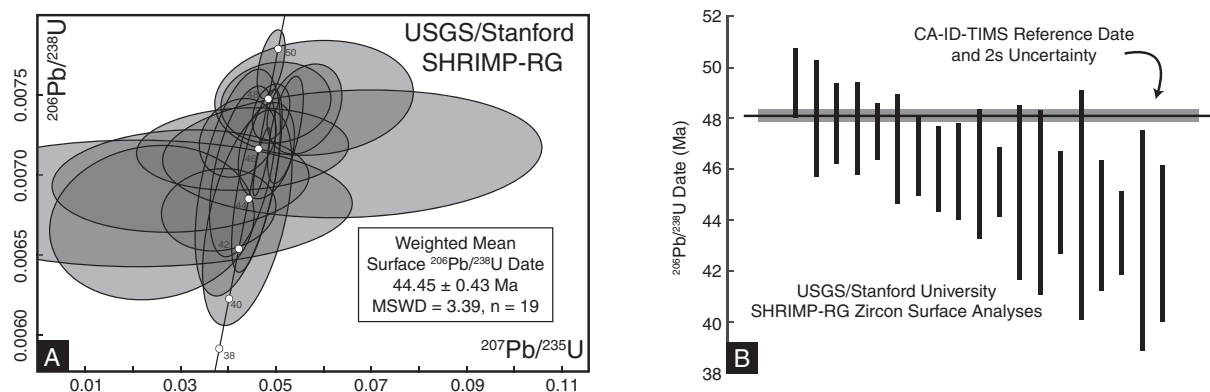

Figure 7. A Wetherill concordia plot (a) and a rank order plot of $^{206}Pb/^{238}U$ dates (b) from analyses of unpolished surfaces (outermost 2 μm) of GHR1 zircon measured by SIMS. The dates show significant scatter and many are younger than the CA-ID-TIMS reference date (b). These younger dates suggest either the presence of younger zircon overgrowths or Pb loss in zircon rims. All uncertainties are reported as 2*s*.

calculate U, Th and Pb mass fractions in unknown samples, and the Temora-2 zircon reference material (Table 1: Black *et al.* 2004) was used to normalise the $^{206}Pb/^{238}U$ ratio. Data reduction follows the methods of Williams (1998) and used the SQUID 2.5 software (Ludwig 2009). All common Pb is assumed to be the result of surface contamination, and isotopic ratios were corrected for this contamination using the measured ^{204}Pb and the modern crustal Pb isotopic composition of Stacey and Kramers (1975). FC1 zircons were used to evaluate reproducibility and eight analyses of

these grains gave a weighted mean $^{207}Pb/^{206}Pb$ date of 1098.8 ± 6.8 (2*s*, MSWD = 1.10), within uncertainty of the reported value (Table 1). The twenty analyses of GHR1 are reported in Table S7 and shown on Figures 5 and 6. Four analyses were discarded due to high Pb$_c$ ($^{206}Pb/^{204}Pb < 1500$). The remaining sixteen analyses are shown in Figure 6 and give a weighted mean $^{206}Pb/^{238}U$ date of 48.70 ± 0.50 (2*s*, MSWD = 1.19), where the uncertainty represents measurement repeatability precision.

Hf isotopic determinations

Solution MC-ICP-MS (MIT)

Trace element solutions from ten zircons (za through zj; Table S1) dated at MIT were collected from chemically abraded zircons following the methods outlined in Schoene et al. (2010). These solutions were split into two aliquots, one for measurement of Hf isotopic composition by MC-ICP-MS and another for trace element mass fractions via quadrupole ICP-MS. Hf was separated from the first set of solutions following methods modified from Goodge and Vervoort (2006) and described in detail in the supplementary material for Eddy et al. (2017). Hf isotopic compositions were measured on a Nu Plasma II-ES MC-ICP-MS at MIT and were bracketed by runs of the JMC-475 standard solution at 25 ng/ml concentration to correct for instrumental bias and to assess reproducibility. Data reduction was done using an 'in-house' spreadsheet. Repeat runs of the JMC-475 standard solution during analyses of GHR1 gave a $^{176}Hf/^{177}Hf = 0.282160 \pm 14$ (2s, n = 13). This value is in good agreement with the published $^{176}Hf/^{177}Hf$ 0.282161 ± 14 from Vervoort and Blichert-Toft (1999). It also provides a good estimate of the reproducibility of $^{176}Hf/^{177}Hf$ measurements produced using solution MC-ICP-MS at MIT. The mean and standard deviation of $^{176}Hf/^{177}Hf$ for all ten analyses of GHR1 is 0.283050 ± 0.000017 (2s) and corresponds to an $\varepsilon Hf_{(0)}$ of +9.4 ± 0.6 (2s: Figure 8 and Table S8). The measurement repeatability precision is similar to the reproducibility of the JMC-475 standard solution, indicating that the $^{176}Hf/^{177}Hf$ of GHR1 is homogenous within measurement precision.

The Lu/Hf ratio of each analysed zircon was measured from a subaliquot of the dissolved zircon solution on an Agilent 7900 quadrupole ICP-MS at MIT using the methods described in the appendix to Eddy et al. (2017). The $^{176}Lu/^{177}Hf$ for each grain was calculated from the measured Lu/Hf using the Lu isotopic composition presented in Vervoort et al. (2004) and used to calculate an initial $^{176}Hf/^{177}Hf$ for each grain using the ^{176}Lu decay constant ($\lambda = 1.867 \times 10^{-11}$ year^{-1}) presented in Söderlund et al. (2004). A mean $\varepsilon Hf_{(i)}$ for all ten analysed zircons of GHR1 is +10.4 ± 0.6 (2s), calculated using the values for CHUR presented in Bouvier et al. (2008).

LA-ICP-MS (Washington State University)

Ten Hf isotopic analyses of GHR1 zircon were conducted at Washington State University by LA-ICP-MS. These analyses used a New Wave Nd:YAG UV 213-nm laser coupled with a Thermo-Finnigan Neptune Multi-Collector ICP-MS and used the methods outlined in Gaschnig et al. (2011). The spot size

was approximately 40 μm in diameter with a depth of ~ 40 μm, and spots were placed independently of analysed U-Pb ablation pits. Mass-dependent fractionation of Hf was corrected by internal normalisation relative to a $^{179}Hf/^{177}Hf = 0.73250$ (Patchett and Tasumoto 1980), using an exponential law. A correction for the isobaric interference between ^{176}Yb and ^{176}Hf was done semi-empirically by monitoring zircon reference materials 91500, FC1 and Mud Tank to calibrate mass bias for Yb and using a $^{176}Yb/^{173}Yb$ adjusted to minimise the offset in the measured $^{176}Hf/^{177}Hf$ in the reference materials as a function of the calculated $^{176}Yb/^{177}Hf$ (e.g., Gaschnig et al. 2011, Ibañez-Mejia et al. 2015). No correction was done for isobaric interference between ^{176}Lu and ^{176}Hf. All data reduction was done using an 'in-house' spreadsheet. Plešovice zircon was used to assess reproducibility and six analyses gave a mean $^{176}Hf/^{177}Hf$ of 0.282472 ± 52 (2s), which is in good agreement with the reference value from Sláma et al. (2008). Ten analyses of GHR1 zircon gave a $^{176}Hf/^{177}Hf$ of 0.283040 ± 44 (2s), corresponding to an $\varepsilon Hf_{(0)}$ of +9.0 ± 1.6 (2s: Figure 8 and Table S9). The initial $^{176}Hf/^{177}Hf$ was calculated using the measured $^{176}Lu/^{177}Hf$, the decay constant for ^{176}Lu ($\lambda = 1.867 \times 10^{-11}$ year^{-1}) presented in Söderlund et al. (2004) and the CA-ID-TIMS crystallisation age for GHR1. A mean $\varepsilon Hf_{(i)}$ for all ten analysed zircons of GHR1 is +10.0 ± 1.5 (2s), calculated using the values for CHUR presented in Bouvier et al. (2008).

LA-ICP-MS (U. Arizona)

The Hf isotopic composition of GHR1 zircon was measured at the University of Arizona Laserchron centre using a Nu Plasma High-Resolution-ICP-MS coupled to a Photon Machines Analyte G2 laser ablation system following methods outlined by Cecil et al. (2011) and Ibañez-Mejia et al. (2014). Ablation pits were placed over pre-existing U-Pb pits and were ~ 40 μm in diameter with pits < 15 μm in depth. Mass numbers 171 through 180 were monitored simultaneously on an array of ten Faraday cups. Mass-dependent fractionation of Hf was corrected using the constant $^{179}Hf/^{177}Hf = 0.73250$ (Patchett and Tasumoto 1980), and Yb fractionation was corrected using the constant $^{173}Yb/^{171}Yb = 1.132338$ (Vervoort et al. 2004) for analyses where the total Yb beam is > 5 mV. For weaker Yb beams, the Hf fractionation factor is applied. The measured $^{176}Hf/^{177}Hf$ was corrected for ($^{176}Lu + ^{176}Yb$) isobaric interferences by monitoring ^{175}Lu and using the natural $^{176}Lu/^{175}Lu = 0.02653$ (Patchett 1983) and the $^{176}Yb/^{171}Yb = 0.901691$ (Vervoort et al. 2004). Machine parameters were tuned at the beginning and end of the session using a 10 ng ml^{-1} solution of JMC-475 with the published $^{176}Hf/^{177}Hf = 0.282161 \pm 14$ (Vervoort and
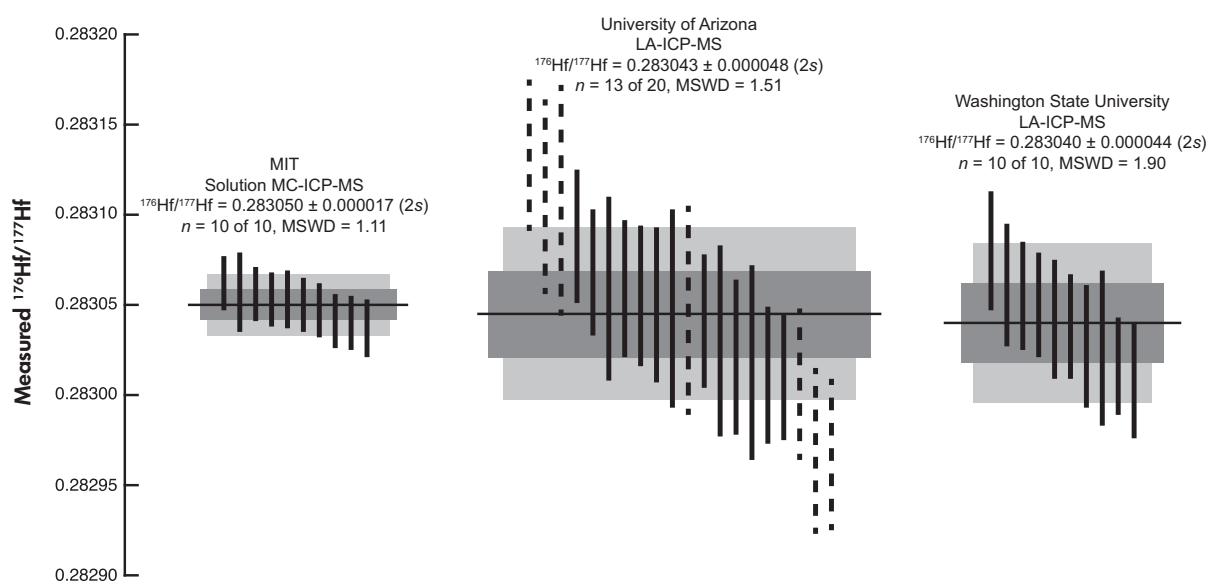
Figure 8. Rank order plot comparing the $^{176}Hf/^{177}Hf$ results from solution multi-collector-inductively coupled plasma-mass spectrometry (MC-ICP-MS) with those from laser ablation (LA)-ICP-MS. The dashed analyses from the University of Arizona contained ($^{176}Lu + ^{176}Yb)/^{176}Hf > 40\%$ and are not included in the calculation of the mean. All uncertainty is reported as 2s.

Blichert-Toft 1999). Additional JMC-475 solutions doped with varying concentrations of Yb and Lu were measured to confirm the efficacy of the corrections used for isobaric interferences. An in-house spreadsheet was used for all data reduction. The $^{176}Hf/^{177}Hf$ of Mud Tank (Table 1: Woodhead and Hergt 2005), Temora-2 (Table 1: Woodhead and Hergt 2005), FC-1 (Table 1: Woodhead and Hergt 2005), 91500 (Table 1: Wiedenbeck et al. 1995, Woodhead and Hergt 2005), Plešovice (Table 1: Sláma et al. 2008), R33 (Table 1: Fisher et al. 2014) and SL2 (Table 1: Woodhead and Hergt 2005) zircon reference materials were analysed during the same session as GHR1 and gave mean $^{176}Hf/^{177}Hf = 0.282518 \pm 0.000056$ (2s), $^{176}Hf/^{177}Hf = 0.282621 \pm 92$ (2s), $^{176}Hf/^{177}Hf = 0.28219 \pm 12$ (2s), $^{176}Hf/^{177}Hf = 0.28228 \pm 10$ (2s), $^{176}Hf/^{177}Hf = 0.282465 \pm 75$ (2s), $^{176}Hf/^{177}Hf = 0.28276 \pm 0.00012$ (2s) and $^{176}Hf/^{177}Hf = 0.283045 \pm 87$ (2s), respectively (Table S10). All of the measured $^{176}Hf/^{177}Hf$ are in good agreement with the published values for these zircon reference materials (Table 1). The mean $^{176}Hf/^{177}Hf$ value for twenty analyses of GHR1 was 0.283045 ± 0.000087 (2s) and corresponds to an $\varepsilon Hf_{(0)}$ of $+9.2 \pm 3.1$ (2s: Figure 8 and Table S10). The full data set contains excess dispersion (MSWD = 3.86), which we attribute to the difficulty of correcting for isobaric interferences in samples with high $(^{176}Yb + ^{176}Lu)/^{176}Hf$ (Figure 7). Excluding the seven analyses with $(^{176}Yb + ^{176}Lu)/^{176}Hf > 40\%$, corresponding to

$(^{176}Yb + ^{176}Lu)/^{176}Hf$ values that greatly exceed those seen in the solution MC-ICP-MS analyses (Figure 9), gives a mean $^{176}Hf/^{177}Hf = 0.283043 \pm 0.000048$ (2s) and reduces the observed dispersion (MSWD = 1.51). The corresponding $\varepsilon Hf_{(0)}$ for this smaller data set is $+9.1 \pm 1.7$ (2s). The initial $^{176}Hf/^{177}Hf$ was calculated for the smaller data set using the measured $^{176}Lu/^{177}Hf$, the decay constant for ^{176}Lu ($\lambda = 1.867 \times 10^{-11}$ year^{-1}) presented in Söderlund et al. (2004) and the CA-ID-TIMS crystallisation age for GHR1. A mean $\varepsilon Hf_{(i)}$ for these thirteen analyses of GHR1 is $+10.1 \pm 1.7$ (2s), calculated using the values for CHUR presented in Bouvier et al. (2008).

Discussion

GHR1 suitability as a natural reference material for microbeam U-Pb analysis of zircon

The excellent agreement between the CA-ID-TIMS U-Pb geochronology from both MIT and Princeton University highlights the utility of the EARTHTIME initiative in minimising interlaboratory bias by establishing common isotopic tracers (Condon et al. 2015, McLean et al. 2015) and data reduction methods for ID-TIMS geochronology (Schmitz and Schoene 2007, McLean et al. 2011). In this case, two independent laboratories produced the same date to within the reported uncertainties of 0.02–0.04%. The twenty-three CA-ID-TIMS $^{206}Pb/^{238}U$ dates for GHR1 zircon also show
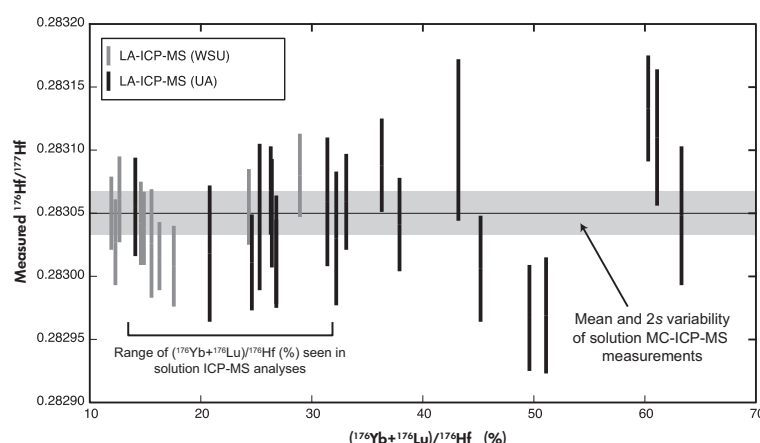
Figure 9. Plot of ^{176}Hf/^{177}Hf for GHR1 measured by LA-ICP-MS compared with the per cent of mass 176 represented by isobaric interferences (^{176}Yb and ^{176}Lu). The plot shows a greater divergence in measured ^{176}Hf/^{177}Hf values from the mean of solution ICP-MS measurements when there are high levels of interference, suggesting that the increased scatter in the LA-ICP-MS data may be related to the difficulty of making interference corrections. The range of (^{176}Yb + ^{176}Lu)/^{176}Hf % measured in the trace element aliquots of the solution analyses is also shown. The greater range of (^{176}Yb + ^{176}Lu)/^{176}Hf % in LA-ICP-MS analyses may reflect analyses that incorporated REE-rich inclusions such as apatite. These inclusions were removed from the solution analyses during the chemical abrasion step. All uncertainty bars are reported at 2s.

that there is little to no intercrystal age dispersion that is resolvable at the reported 2s uncertainty (Figure 3). This observation is consistent with the interpretation that the rapakivi intrusive phase of the Golden Horn batholith rapidly intruded and crystallised without prolonged ($\gg$ 100 ky) melt residence (Eddy *et al.* 2016). The two older analyses produced at Princeton University suggest that rare older grains exist within the GHR1 granite. These grains were likely recycled from older parts of the magmatic system, but are rare. In this study, they represent 8% of the total number of grains analysed by CA-ID-TIMS. In both cases, the grains were significantly older (1–4%) than the recommended reference value and can be easily identified during CA-ID-TIMS analysis. Nevertheless, the excellent agreement between independent laboratories and the apparent lack of age dispersion in CA-ID-TIMS ^{206}Pb/^{238}U dates further suggests that GHR1 zircon will be useful as a reference material for U-Pb zircon CA-ID-TIMS geochronology.

Microbeam U-Pb analyses from GHR1 zircon show that the ^{206}Pb/^{238}U date is reproducible across several laboratories using different analytical methods (Figure 6). However, our study reveals four potential limitations to consider when using GHR1 as a reference material. (1) Like most Cenozoic zircon, GHR1 has low total Pb mass fraction. (2) GHR1 zircon contains abundant inclusions that may contain high Pb$_c$. (3) A spread in ages of whole grain dissolutions without using chemical abrasion (Figure 4) and in zircon surface analyses

by SIMS (Figure 7) suggests the presence of either younger overgrowths or Pb loss. (4) The presence of xenocrysts up to 4% older than the main zircon population, which may bias weighted means of GHR1. We consider all of the limitations listed above to preclude the use of GHR1 as a primary reference material for calibration of U-Pb isotopic measurements during microbeam analyses. Likewise, the variable U mass fraction (150–2000 µg g^{-1} with outliers $\gg$ 2000 µg g^{-1}: Tables S3–S7), variable REE mass fractions (Figure 11 and Table S11) and the presence of REE-bearing inclusions preclude the use of GHR1 for calibration of elemental mass fractions in zircon during microbeam analyses (Figure 11). However, our data demonstrate the reproducibility of the ^{206}Pb/^{238}U ratio in GHR1 zircon interiors across a variety of methods, and all participating laboratories produced dates that are in agreement with the CA-ID-TIMS reference date for GHR1 to within < 1–1.5% (Figure 6 and Table 2). Given the apparent homogeneity of ^{206}Pb/^{238}U in GHR1 grain interiors, we suggest that it will provide a useful secondary reference material for assessing the accuracy of fractionation correction and reproducibility of microbeam U-Pb geochronology of Cenozoic zircon. In this capacity, the intercrystal variability in U and REE mass fractions will provide an important check on corrections related to variable matrix composition (e.g., Black *et al.* 2004, Jackson *et al.* 2004) and variable amounts of radiation damage (e.g., Steely *et al.* 2014, Sliwinski *et al.* 2017). Below we offer guidelines for how to best utilise GHR1 zircon in this capacity.

The systematically younger $^{206}Pb/^{238}U$ dates for zircons analysed by ID-TIMS without chemical abrasion (Figure 4) and SIMS surface analyses (Figure 7) suggest some degree of Pb loss or younger overgrowths in GHR1 zircon. We do not think that these dates incorporate younger zircon growth, because no obvious overgrowths were observed in cathodoluminescence images (Figure 2) and there are no documented magmatic or metamorphic events after 47.729 Ma in the Golden Horn batholith (Eddy *et al.* 2016). Instead, Pb-loss is a more likely explanation for these anomalously young dates. We consider that this Pb loss is concentrated in the zircon rims because most microbeam analyses of GHR1 zircon interiors reproduced the reference CA-ID-TIMS date (Figure 6), while nearly all of the SHRIMP-RG analyses of zircon surfaces (outermost ~ 2 μm) yielded younger dates (Figure 7). A comparison of U mass fractions measured from grain interiors and surfaces on the SHRIMP-RG at the Stanford University/USGS laboratory also indicates that the surfaces have higher average U content than interiors, and thus, more radiation damage (Table S6). Therefore, we recommend that microbeam analyses of GHR1 zircon avoid zircon edges to reduce the possibility of incorporating zones that could include Pb loss.

High Pb$_c$ in some microbeam zircon analyses of GHR1 interiors resulted in $^{206}Pb/^{238}U$ dates that significantly deviate from the CA-ID-TIMS reference date. We attribute this deviation to the challenges of accurately measuring $^{206}Pb/^{204}Pb$ during microbeam analyses and budgeting the Pb$_c$ composition between the composition expected in co-crystallised inclusions and the composition of Pb in modern surficial contamination. These challenges make it difficult to accurately correct isotopic ratios for Pb$_c$ contamination and can result in spurious dates. Figure 10 shows the deviation from the CA-ID-TIMS reference date of all $^{206}Pb/^{238}U$ dates produced during microbeam analyses of GHR1 grain interiors relative to measured $^{206}Pb/^{204}Pb$. Increased deviation from the reference value occurs at $^{206}Pb/^{204}Pb$ < 1500.

Consequently, we recommend that microbeam analyses of GHR1 zircon be discarded if $^{206}Pb/^{204}Pb$ < 1500. Using CL or BSE images to avoid inclusions during microbeam analyses may also help increase the number of spots that meet this condition, as the presence of Pb$_c$-bearing inclusions is inferred from the elevated Pb$_c$ observed in the ID-TIMS analyses that did not undergo chemical abrasion (Table S2).

The occurrence of older ante- or xenocrystic zircon in GHR1 is highlighted by the two CA-ID-TIMS analyses that were ~ 1% and ~ 4% older than the main zircon population (Table S2). The incorporation of older zircon is common in magmatic systems, and these grains likely reflect cannibalisation of zircon from older wall rock. Similar incorporation of ante- or xenocrystic zircon has been identified in ID-TIMS analyses of other natural zircon reference materials (R33: Black *et al.* 2004, Penglai: Li *et al.* 2010) and will likely be a persistent problem in zircon reference materials separated from igneous rocks rather than subsampled from large, homogeneous zircon megacrysts. These older grains will be easily identified in CA-ID-TIMS analyses, as they are distinctly older than the main age population. However, the identification of ante- or xenocrysts that are < 4% older than the reference age during microbeam analyses is more difficult. Due to the presence of these grains, we recommend that several different individual zircons are analysed during a session and that any grain that consistently produces an older age is excluded. The internal structure of the two older zircon analysed by CA-ID-TIMS was not documented with CL or BSE images prior to dissolution. Future CA-ID-TIMS analyses coupled with CL or BSE images may identify features that can be used during microbeam analyses to avoid these grains. Nevertheless, the good agreement between large-n microbeam U-Pb geochronological data sets and the CA-ID-TIMS reference date suggests that the limited presence of ante- or xenocrystic grains does not have a major effect on these analyses at the current level of age precision that is achievable by LA-ICP-MS and SIMS.

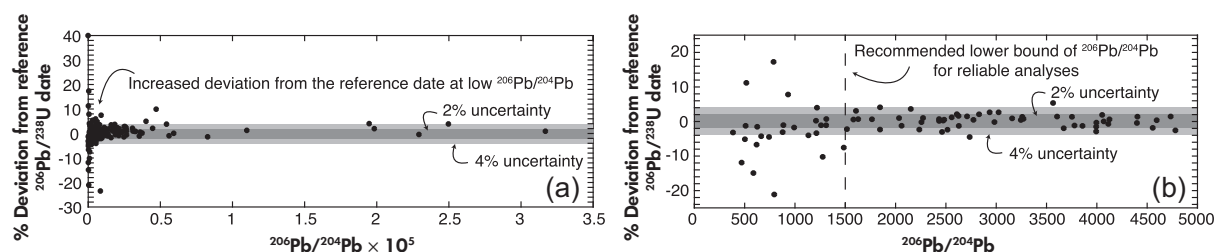**Figure 10. The % deviation from the CA-ID-TIMS reference date of microbeam analyses compared with the analysed $^{206}Pb/^{204}Pb$. The full data set is shown in (a), while (b) highlights the analyses with the lowest $^{206}Pb/^{204}Pb$. We notice a marked increase in deviation from the reference date at low $^{206}Pb/^{204}Pb$ and recommend that analyses with $^{206}Pb/^{204}Pb$ < 1500 be treated as unreliable.**

Table 3.
Summary of Hf isotopic results

Laboratory	Method [a]	No. of analyses	$^{176}Hf/^{177}Hf$	2s	MSWD [b]	$\varepsilon Hf_{(0)}$
MIT	Solution MC-ICP-MS	n = 10 of 10	0.283050	0.000017	1.11	9.4
Washington State University	LA-ICP-MS	n = 10 of 10	0.283040	0.000044	1.90	9.0
University of Arizona	LA-ICP-MS	n = 13 of 20	0.283043	0.000048	1.51	9.1

[a] Solution MC-ICP-MS: solution multi-collector-inductively coupled plasma-mass spectrometry, LA-MC-ICP-MS: laser ablation-multi-collector-inductively coupled plasma-mass spectrometry.
[b] Mean square weighted deviation (Wendt and Carl 1992). Calculated using the MATLAB script in the Appendix S1.
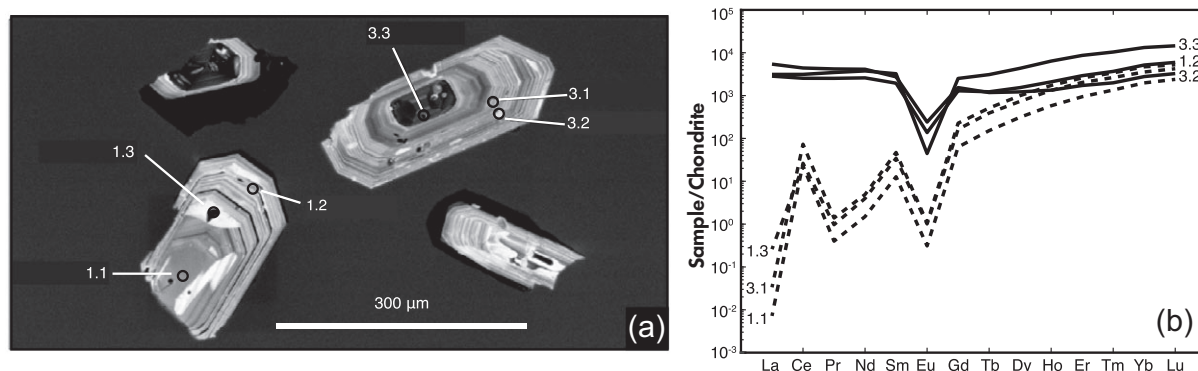

Figure 11. (a) CL image showing the location of spots analysed for REE mass fractions at São Paulo University. (b) Chondrite normalised (using the values reported in McDonough and Sun 1995) rare earth element (REE) spider plots of spots analysed on GHR1 zircons. Elevated REE content (1.2, 3.2 and 3.3), relative to the content seen in 'clean' zircon (1.1, 1.3, 3.1), is correlated with the presence of inclusions in the analysed volume. However, given that the matrix of inclusion-bearing analyses (1.2, 3.2, 3.3) differs from the reference material (91500 zircon: Wiedenbeck *et al.* 2004) used to calculate the sensitivity factor between NIST 610 glass and zircon, we emphasise that these measurements should only be considered qualitative. Energy-dispersive X-ray spectroscopy (EDS) measurements of these inclusions identified them as apatite. REE analyses follow the methods of Sato *et al.* (2016) and are reported in Table S11.

Despite the potential limitations of GHR1 zircon, the homogeneity of the $^{206}Pb/^{238}U$ ratio in zircon interiors (Figure 6) suggests that it can be a useful secondary reference material. In this respect, the 48.106 ± 0.023 Ma age of GHR1 is important because Cenozoic zircon reference materials for microbeam U-Pb geochronological analyses (Table 1) are currently limited to a single 38.896 ± 0.012 Ma gem-quality zircon crystal (Kennedy *et al.* 2014) and *ca.* 4.4 Ma zircon megacrysts from an alkaline basalt (Li *et al.* 2010) and zircon separated from the Fish Canyon Tuff (Schmitz and Bowring 2001, Wotzlaw *et al.* 2013) that show significant age heterogeneity in ID-TIMS analyses. Thus, the well-characterised age of GHR1 zircon and its practically unlimited supply will help fill this role as the use of microbeam methods for dating Cenozoic igneous and detrital zircons becomes increasingly common.

Suitability as a natural reference material for microbeam Hf isotope determinations in zircon

The variability seen in solution MC-ICP-MS measurements of $^{176}Hf/^{177}Hf$ from GHR1 zircon is similar to the variability reported for in repeat measurements of the JMC-475 Hf isotopic standard solution, suggesting that there is no resolvable intercrystal variability in $^{176}Hf/^{177}Hf$. Consequently, we recommend using our mean $^{176}Hf/^{177}Hf$ = 0.283050 ± 17 (2s) from solution MC-ICP-MS analyses as a reference Hf isotopic value for GHR1 zircon. The mean $^{176}Hf/^{177}Hf$ values measured by both LA-ICP-MS laboratories are in good agreement with this value, demonstrating that it is reproducible by microbeam methods (Figure 8 and Table 3).

Ytterbium and Lu mass fractions from some of the University of Arizona LA-ICP-MS measurements also far

exceed those seen in the solution measurements (Figure 9). We attribute this difference to ablation of zircon with elevated REE content or by contamination of the analysis by REE-bearing inclusions during the laser ablation process. The possibility for high U domains along grain rims may suggest late zircon growth from an evolved liquid that would likely have correspondingly high REE content. Dissolution of these zones during the chemical abrasion process may explain the more restricted range of Yb and Lu seen in the trace element measurements from MIT. Alternatively, ablation of REE-bearing inclusions may be responsible for the elevated REE content observed in some of the microbeam ^{176}Hf/^{177}Hf measurements (Figure 11). The removal of these inclusions during chemical abrasion would also explain the lower mass fractions of REE seen in the MIT analyses. Given the ubiquity of inclusions in the GHR1 zircons, the possibility of high REE growth zones, and the difficulty in correcting for isobaric interferences from REE (e.g., ^{176}Yb and ^{176}Lu) during the measurement of ^{176}Hf/^{177}Hf, we suggest that all grains used as reference material for ^{176}Hf/^{177}Hf measurements be imaged prior to analysis so that both inclusions and grain exteriors can be avoided during targeting. Additional screening of analyses with high measured Yb and Lu (i.e., ^{176}(Yb + Lu)/^{176}Hf > 40%) may also be effective for removing analyses that yield anomalous ^{176}Hf/^{177}Hf values due to excess REE incorporated from inclusions. Regardless, the ^{176}Hf/^{177}Hf = 0.283050 ± 17 (2s, εHf$_{(0)}$ = +9.3) of GHR1 zircon is the most radiogenic Hf isotopic composition in any available zircon reference material (Table 1) and should be useful in assessing the reproducibility of analyses of zircon with high εHf$_{(0)}$.

Conclusions

Zircon from sample GHR1 is characterised by homogeneous U-Pb and Hf isotopic systematics as evidenced by the highly reproducible ^{206}Pb/^{238}U and ^{176}Hf/^{177}Hf by CA-ID-TIMS and solution MC-ICP-MS, respectively. These values are also reproducible by microbeam techniques (LA-ICP-MS and SIMS). The age and geochemical reproducibility, potentially inexhaustible supply, 48.106 ± 0.023 Ma age and radiogenic εHf$_{(0)}$ all suggest that GHR1 will provide a useful reference material for assessing reproducibility of U-Pb analyses of Cenozoic zircon and radiogenic ^{176}Hf/^{177}Hf during microbeam analyses. However, care must be taken to avoid analysing REE- and Pb$_c$-bearing inclusions and zircon edges where Pb loss may have occurred. Zircon separates from this sample are available to interested laboratories through the corresponding authors.

References

Bauer A.M., Fisher C.M., Vervoort J.D. and Bowring S.A. (2017)
Coupled zircon Lu-Hf and U-Pb isotopic analyses of the oldest terrestrial crust, the >4.03 Ga Acasta Gneiss Complex. Earth and Planetary Science Letters, 458, 37–48.

Black L.P. and Gulson B.L. (1978)
The age of the mud tank carbonatite, strangeways range, Northern Territory. BMR Journal of Australian Geology and Geophysics, 3, 227–232.

Black L.P., Kamo S.L., Allen C.M., Aleinikoff J.N., Davis D.W., Korsch R.J. and Foudoulis C. (2003)
TEMORA-1: A new zircon standard for Phanerozoic U-Pb geochronology. Chemical Geology, 200, 155–170.

Black L.P., Kamo S.L., Allen C.M., Davis D.W., Aleinikoff J.N., Valley J.W., Mundil R., Campbell I.H., Korsch R.J., Williams I.S. and Foudoulis C. (2004)
Improved ^{206}Pb/^{238}U microprobe geochronology by the monitoring of a trace-element-related matrix effect: SHRIMP, ID-TIMS, ELA-ICP-MS and oxygen isotope documentation for a series of zircon standards. Chemical Geology, 205, 115–140.

Bouvier A., Vervoort J.D. and Patchett J.D. (2008)
The Lu-Hf and Sm-Nd isotopic composition of CHUR: Constraints from unequilibrated chondrites and implications for the bulk composition of terrestrial planets. Earth and Planetary Science Letters, 273, 48–57.

Bowring J.F., McLean N.M. and Bowring S.A. (2011)
Engineering cyber infrastructure for U-Pb geochronology: Tripolig and U-Pb_Redux. Geochemistry, Geophysics, Geosystems, 12, Q0AA19.

Cecil M.R., Gehrels G., Ducea M.N. and Patchett P.J. (2011)
U-Pb-Hf characterization of the central Coast Mountains batholith: Implications for petrogenesis and crustal architecture. Lithosphere, 3, 247–260.

Chang Z., Vervoort J.D., McClelland W.C. and Knaack C. (2006)
U-Pb dating of zircon by LA-ICP-MS. Geochemistry, Geophysics, Geosystems, 7, Q05009.

references

Coble M.A., Vazquez J.A., Barth A.P., Wooden J., Burns D., Kylander-Clark A., Jackson S. and Vennari C.E. (2018)
Trace element characterisation of MAD-559 zircon reference material for ion microprobe analysis. **Geostandards and Geoanalytical Research**, 42, 481–497.

Condon D.J., Schoene B., McLean N.M., Bowring S.A. and Parrish R.R. (2015)
Metrology and traceability of U-Pb isotopic dilution geochronology (EARTHTIME tracer calibration part I). **Geochimica et Cosmochimica Acta**, 164, 464–480.

Dhuime B., Hawkesworth C.J., Cawood P.A. and Storey C.D. (2012)
A change in the geodynamics of continental growth 3 billion years ago. **Science**, 335, 1334–1336.

Eddy M.P., Bowring S.A., Miller R.B. and Tepper J.H. (2016)
Rapid assembly and crystallization of a fossil large-volume silicic magma chamber. **Geology**, 44, 331–334.

Eddy M.P., Jagoutz O. and Ibañez-Mejia M. (2017)
Timing of initial seafloor spreading in the Newfoundland-Iberia rift. **Geology**, 45, 527–530.

Fisher C.M., Vervoort J.D. and Hanchar J.M. (2014)
Guidelines for reporting zircon Hf isotopic data by LA-MC-ICP-MS and potential pitfalls. **Chemical Geology**, 363, 125–133.

Gaschnig R.M., Vervoort J.D., Lewis R.S. and Tikoff B. (2011)
Isotopic evolution of the Idaho batholith and Challis intrusive province, northern US Cordillera. **Journal of Petrology**, 52, 2397–2429.

Gehrels G.E. (2014)
Detrital zircon U-Pb geochronology applied to tectonics. **Annual Review of Earth and Planetary Sciences**, 42, 127–149.

Gehrels G.E., Valencia V. and Ruiz J. (2008)
Enhanced precision, accuracy, efficiency, and spatial resolution of U-Pb ages by laser ablation-multi-collector-inductively coupled plasma-mass spectrometry. **Geochemistry, Geophysics, Geosystems**, 9, Q03017.

Goodge J.W. and Vervoort J.D. (2006)
Origin of mesoproterozoic A-type granites in Laurentia: Hf isotope evidence. **Earth and Planetary Science Letters**, 243, 711–731.

Guillong M., von Quadt A., Sakata S., Peytcheva I. and Bachmann O. (2014)
LA-ICP-MS Pb-U dating of young zircons from the Kos-Nisyros volcanic centre, SE Aegean arc. **Journal of Analytical Atomic Spectrometry**, 29, 963–970.

Hiess J., Condon D.J., McLean N.M. and Noble S.R. (2012)
$^{238}U/^{235}U$ systematics in terrestrial uranium-bearing minerals. **Science**, 335, 1610–1614.

Horstwood M.S.A., Košler J., Gehrels G., Jackson S.E., McLean N.M., Paton C., Pearson N.J., Sircombe K., Sylvester P., Vermeesch P., Bowring J.F., Condon D.J. and Schoene B. (2016)
Community-derived standards for LA-ICP-MS U-(Th-)Pb geochronology – Uncertainty propagation, age interpretation and data reporting. **Geostandards and Geoanalytical Research**, 40, 311–332.

Ibañez-Mejia M., Gehrels G.E., Ruiz J., Vervoort J.D., Eddy M.P. and Li C. (2014)
Small-volume baddeleyite (ZrO_2) U-Pb geochronology and Lu-Hf isotope geochemistry by LA-ICP-MS: Techniques and applications. **Chemical Geology**, 384, 149–167.

Ibañez-Mejia M., Pullen A., Arenstein J., Gehrels G.E., Valley J., Ducea M.N., More A.R., Pecha M. and Ruiz J. (2015)
Unravelling crustal growth and reworking processes in complex zircons from orogenic lower-crust: The Proterozoic Putumayo Orogen of Amazonia. **Precambrian Research**, 267, 285–310.

Ickert R.B., Hiess J., Williams I.S., Holden P., Ireland T.R., Lanc P., Schram N., Foster J.J. and Clement S.W. (2008)
Determining high precision, *in situ*, oxygen isotope ratios with a SHRIMP II: Analyses of MPI-DING silicate-glass reference materials and zircon from contrasting granites. **Chemical Geology**, 257, 114–128.

Ireland T.R. and Williams I.S. (2003)
Considerations in zircon geochronology by SIMS. In: Hanchar J.M. and Hoskin P.W.O. (eds), Zircon: Reviews in Mineralogy and Geochemistry, 53, 215–241.

Jackson S.E., Pearson N.J., Griffin W.L. and Belousova E.A. (2004)
The application of laser ablation-inductively couples plasma-mass spectrometry to *in situ* U-Pb zircon geochronology. **Chemical Geology**, 211, 47–69.

Kennedy A.K., Wotzlaw J.F., Schaltegger U., Crowley J.L. and Schmitz M. (2014)
Eocene zircon reference material for microanalysis of U-Th-Pb isotopes and trace elements. **The Canadian Mineralogist**, 52, 409–421.

Kita N.T., Ushikubo T., Fu B. and Valley J.W. (2009)
High precision SIMS oxygen isotope analysis and the effect of sample topography. **Chemical Geology**, 264, 43–57.

Li X.H., Liu Y., Li Q.L., Guo C.H. and Chamberlain K.R. (2009)
Precise determination of Phanerozoic zircon Pb/Pb age by multicollector SIMS without external standardization. **Geochemistry, Geophysics, Geosystems**, 10, Q04010.

references

Li Q.L., Li X.H., Liu Y., Tang G.Q., Yang J.H. and Zhu W.G. (2010)
Precise U-Pb and Pb-Pb dating of Phanerozoic baddeleyite by SIMS with oxygen flooding technique. **Journal of Analytical Atomic Spectrometry**, 25, 1107–1113.

Li X.H., Tang G.Q., Gong B., Yang Y.H., Hou K.J., Hu Z.C., Li Q.L., Liu Y. and Li W.X. (2013)
Qinghu zircon: A working reference for microbeam analysis of U-Pb age and Hf and O isotopes. **Chinese Science Bulletin**, 58, 4647–4654.

Ludwig K.W. (2009)
SQUID 2: A user's manual. **Berkeley Geochronology Center Special Publication** 5, 110pp.

Matthews N.E., Vazquez J.A. and Calvert A.T. (2015)
Age of the Lava Creek supereruption and magma chamber assembly at Yellowstone based on $^{40}Ar/^{39}Ar$ and U-Pb dating of sanidine and zircon crystals. **Geochemistry, Geophysics, Geosystems**, 16, 2508–2528.

Mattinson J.M. (2005)
Zircon U-Pb chemical abrasion ("CA-TIMS") method: Combined annealing and multi-step partial dissolution analysis for improved precision and accuracy of zircon ages. **Chemical Geology**, 220, 47–66.

Mattinson J.M. (2010)
Analysis of the relative decay constants of ^{235}U and ^{238}U by multi-step CA-TIMS measurements of closed system natural zircon samples. **Chemical Geology**, 275, 186–198.

McDonough W.F. and Sun S.S. (1995)
The composition of the Earth. **Chemical Geology**, 120, 223–253.

McLean N.M., Bowring J.F. and Bowring S.A. (2011)
An algorithm for U-Pb isotope dilution data reduction and uncertainty propagation. **Geochemistry, Geophysics, Geosystems**, 12, Q0AA18.

McLean N.M., Condon D.J., Schoene B. and Bowring S.A. (2015)
Evaluating uncertainties in the calibration of isotopic reference materials and multi-element isotopic tracers (EARTHTIME tracer calibration II). **Geochimica et Cosmochimica Acta**, 164, 481–501.

Miller R.B., Paterson S.R., DeBari S.M. and Whitney D.L. (2000)
North Cascades Cretaceous crustal section: Changing kinematics, rheology, metamorphism, pluton emplacement and petrogenesis from 0 to 40 km depth. In: Woodsworth G.J., Jackson J.L.E., Nelson J.L. and Ward B.C. (eds), **Guidebook for geological field trips in southwestern British Columbia and northern Washington. Geological Association of Canada (Vancouver)**, 229–278.

Morel M.L.A., Nebel O., Nebel-Jacobsen Y.J., Miller J.S. and Vroon P.Z. (2008)
Hafnium isotope characterization of the GJ-1 zircon reference material by solution and laser-ablation MC-ICPMS. **Chemical Geology**, 255, 231–235.

Paces J.B. and Miller J.D. Jr (1993)
Precise U-Pb ages of Duluth Complex and related mafic intrusions, northeastern Minnesota: Geochronological insights to physical, petrogenetic, paleomagnetic, and tectonomagmatic processes associated with the 1.1 Ga Midcontinent Rift System. **Journal of Geophysical Research**, 98, 13997–14013.

Padilla A.J., Miller C.F., Carley T.L., Economos R.C., Schmitt A.K., Coble M.A., Wooden J.L., Fisher C.M., Vervoort J.D. and Hanchar J.M. (2016)
Elucidating the magmatic history of the Austurhorn silicic intrusive complex (Southeast Iceland) using zircon elemental and isotopic geochemistry and geochronology. **Contributions to Mineralogy and Petrology**, 171, 69.

Patchett J.P. (1983)
Importance of the Lu-Hf isotopic system in studies of planetary chronology and chemical evolution. **Geochimica et Cosmochimica Acta**, 47, 81–91.

Patchett P.J. and Tasumoto M. (1980)
A routine high-precision method for Lu-Hf isotope geochemistry and chronology. **Contributions to Mineralogy and Petrology**, 75, 263–267.

Pullen A., Ibanez-Mejia M., Gehrels G.E., Giesler D. and Pecha M. (2018)
Optimization of a laser ablation-single collector-inductively coupled plasma-mass spectrometer (Thermo Element 2) for accurate, precise, and efficient zircon U-Th-Pb geochronology. **Geochemistry, Geophysics, Geosystems**, 19, 3689–3705.

Roberts N.M.W. and Spencer C.J. (2015)
The zircon archive of continent formation through time. In: Roberts N.M.W., Van Kranendonk M., Parman S., Shirey S. and Clift P.D. (eds), **Continent formation through time. Geological Society of London Special Publication**, 389, 197–225.

Samperton K.M., Schoene B., Cottle J.M., Keller C.B., Crowley J.L. and Schmitz M.D. (2015)
Magma emplacement, differentiation and cooling in the middle crust: integrated zircon geochronological-geochemical constraints from the Bergell Intrusion, Central Alps. **Chemical Geology**, 417, 322–340.

Sato K., Tassinari C.C.G., Basei M.A.A., Onoe A.T. and Siga O. Jr (2016)
First REE analyses by SHRIMP at Geosciences Institute of São Paulo University: REE diffusion from apatite inclusion inside Temora zircon. **International SHRIMP Workshop**, 8, 71.

Schärer U. (1984)
The effect of initial ^{230}Th disequilibrium on young U-Pb ages: The Makalu case, Himalaya. **Earth and Planetary Science Letters**, 67, 191–204.

Schmitz M.D. and Bowring S.A. (2001)
U-Pb zircon and titanite systematics of the Fish Canyon Tuff: An assessment of high-precision U-Pb geochronology and its application to young volcanic rocks. **Geochimica et Cosmochimica Acta**, 65, 2571–2587.

references

Schmitz M.D. and Schoene B. (2007)
Derivation of isotope ratios, errors, and error correlations for U-Pb geochronology using ^{205}Pb-^{235}U-(^{233}U)-spiked isotope dilution thermal ionization mass spectrometric data. Geochemistry, Geophysics, Geosystems, 8, Q08006.

Schoene B., Latkoczy C., Schaltegger U. and Günther D. (2010)
A new method integrating high-precision U-Pb geochronology with zircon trace element analysis (U-Pb TIMS-TEA). Geochimica et Cosmochimica Acta, 74, 7144–7159.

Sláma J., Košler J., Condon D.J., Crowley J.L., Gerdes A., Hanchar J.M., Horstwood M.S.A., Morris G.A., Nasdala L., Norberg N., Schaltegger U., Schoene B., Tubrett M.N. and Whitehouse M.J. (2008)
Plešovice zircon – A new natural reference material for U-Pb and Hf isotopic microanalysis. Chemical Geology, 249, 1–35.

Sliwinski J.T., Guillon M., Liebske C., Dunkl I., von Quadt A. and Bachmann O. (2017)
Improved accuracy of LA-ICP-MS U-Pb ages of Cenozoic zircons by alpha dose correction. Chemical Geology, 472, 8–21.

Söderlund U., Patchett P.J., Vervoort J.D. and Isachsen C.E. (2004)
The 176Lu decay constant determined by Lu-Hf and U-Pb isotope systematics of Precambrian mafic intrusions. Earth and Planetary Science Letters, 219, 311–324.

Stacey J.S. and Kramers J.D. (1975)
Approximation of terrestrial lead isotope evolution by a two-stage model. Earth and Planetary Science Letters, 26, 207–221.

Steely A.N., Hourigan J.K. and Juel E. (2014)
Discrete multi-pulse laser ablation depth profiling with a single-collector ICP-MS: Sub-micron U-Pb geochronology of zircon and the effect of radiation damage on depth-dependent fractionation. Chemical Geology, 372, 92–108.

Stelten M.E., Cooper K.M., Vazquez J.A., Calvert A.T. and Glessner J.J.G. (2015)
Mechanisms and timescales of generating eruptible rhyolitic magmas at Yellowstone caldera from zircon and sanidine geochronology and geochemistry. Journal of Petrology, 56, 1607–1642.

Stern R.A. and Amelin Y. (2003)
Assessment of errors in SIMS zircon U-Pb geochronology using a natural zircon standard and NIST SRM 610 glass. Chemical Geology, 197, 111–142.

Stern R.A., Bodorkos S., Kama S.L., Hickman A.H. and Corfu F. (2009)
Measurement of SIMS instrumental mass fractionation of Pb isotopes during zircon dating. Geostandards and Geoanalytical Research, 33, 145–168.

Stull R.J. (1969)
The geochemistry of the southeastern portion of the Golden Horn batholith, Northern Cascades, Washington. PhD thesis, University of Washington (Seattle, USA) 127pp.

Stull R.J. (1978)
Mantled feldspars from the Golden Horn batholith, Washington. Lithos, 11, 243–249.

Vervoort J.D. and Blichert-Toft J. (1999)
Evolution of the depleted mantle: Hf isotope evidence from juvenile rocks through time. Geochimica et Cosmochimica Acta, 63, 533–556.

Vervoort J.D., Patchett P.J., Söderlund U. and Baker M. (2004)
Isotopic composition of Yb and the determination of Lu concentrations and Lu/Hf ratios by isotope dilution using MC-ICPMS. Geochemistry, Geophysics, Geosystems, 5, Q11002.

Viete D.R., Kylander-Clark A.R.C. and Hacker B.R. (2015)
Single-shot laser ablation split stream (SS-LASS) petrochronology deciphers multiple, short-duration metamorphic events. Chemical Geology, 415, 70–86.

Vorhies S.H., Ague J.J. and Schmitt A.K. (2013)
Zircon growth and recrystallization during progressive metamorphism, Barrovian zones, Scotland. American Mineralogist, 98, 219–230.

Wendt I. and Carl C. (1991)
The statistical distribution of the mean square weighted deviation. Chemical Geology, 86, 275–285.

Wiedenbeck M., Allé P., Corfu F., Griffin W.L., Meier M., Oberli F., von Quadt A., Roddick J.C. and Spiegel W. (1995)
Three natural zircon standards for U-Th-Pb, Lu-Hf, trace element and REE analysis. Geostandards Newsletter, 19, 1–23.

Wiedenbeck M., Hanchar J.M., Peck W.H., Sylvester P., Valley J., Whitehouse M., Kronz A., Morishita Y., Nasdala L., Fiebig J., Franchi I., Girard J.P., Greenwood R.C., Hinton R., Kita N., Mason P.R.D., Norman M., Ogasawara M., Piccoli P.M., Rhede D., Satoh H., Schultz-Dobrick B., Skar O., Spicuzza M.J., Terada K., Tindle A., Togashi S., Vennemann T., Xie Q. and Zheng Y.F. (2004)
Further characterization of the 91500 zircon crystal. Geostandards and Geoanalytical Research, 28, 9–39.

Williams I.S. (1998)
U-Th-Pb geochronology by ion microprobe. Reviews in Economic Geology, 7, 1–35.

Woodhead J.D. and Hergt J.M. (2005)
A preliminary appraisal of seven natural zircon reference materials for in situ Hf isotope determination. Geostandards and Geoanalytical Research, 29, 183–195.

Wotzlaw J.F., Schaltegger U., Frick D.A., Dungan M.A., Gerdes A. and Günther D. (2013)
Tracking the evolution of large-volume silicic magma reservoirs from assembly to supereruption. Geology, 41, 867–870.

references

Wu F.Y., Yang Y.H., Xie L.W., Yang J.H. and Xu P. (2006)
Hf isotopic compositions of the standard zircons and baddeleyites used in U-Pb geochronology. **Chemical Geology**, 234, 105–126.

Zimmerer M.J., Lafferty J. and Coble M.A. (2016)
The eruptive and magmatic history of the youngest pulse of volcanism at the Valles caldera: Implications for successfully dating late Quaternary eruptions. **Journal of Volcanology and Geothermal Research**, 310, 50–57.

Supporting information

The following supporting information may be found in the online version of this article:

Appendix S1. MATLAB code for U-Pb calculations.

Tables S1–S7. U-PB isotopic data for GHR1 from participating laboratories.

Tables S8–S10. Hf isotopic data of GHR1 single zircons from participating laboratories.

Table S11. SHRIMP REE determinations (University of Sao Paulo).

This material is available at: http://onlinelibrary.wiley.com/doi/10.1111/ggr.12246/abstract (This link will take you to the article abstract).